

## MODELLING STUDY ON THE EFFECT OF ASH FUSION CHARACTERISTICS ON THE BIOMASS SLAGGING BEHAVIOR

by

**Yiming ZHU<sup>a</sup>, Houzhang TAN<sup>a\*</sup>, Yanqing NIU<sup>a</sup>, Yibin WANG<sup>a</sup>,  
Hrvoje MIKULCIC<sup>b</sup>, Milan VUJANOVIC<sup>b</sup>, and Neven DUIC<sup>b</sup>**

<sup>a</sup> MOE Key Laboratory of Thermo-Fluid Science and Engineering, Xi'an Jiaotong University, Xi'an, China

<sup>b</sup> Department of Energy, Power Engineering and Environment, Faculty of Mechanical Engineering and Naval Architecture, University of Zagreb, Zagreb, Croatia

Original scientific paper  
<https://doi.org/10.2298/TSCI171229268Z>

*Ash fusion characteristics of biomass have significant effect on slagging. In this work, the effects of ash fusion characteristics on slagging have been studied by ash fusion experiments and CFD modelling. Based on the basic ash composition of biomass, the mixture of silicon dioxide, calcium oxide, potassium oxide, and aluminum oxide have been selected as simulated ashes for ash fusion characteristics investigation. The results indicate that deformation temperature decreases with increased potassium oxide. High content of calcium oxide and silicon dioxide increase deformation temperature for the skeleton effect, respectively. The reactions of potassium oxide, calcium oxide and silicon dioxide lead to low melting products and decrease deformation temperature. Aluminum oxide increases deformation temperature by forming Si-Al-K compounds while K content is high and decreases deformation temperature while Ca or Si content is high due to the Si-Al-Ca compounds. On basis of the experimental results, an ash particle adhesion model has been developed using the corresponding characteristic temperatures of adhesion. Combined with the deposition model of inertial impaction, a CFD modelling study of ash deposition on heating surface has been performed. For a kind of cotton straw ash with low melting temperature, the modelling results indicate that adhesion of molten ash plays a major role during slagging. The accretion rate of molten ash adhesion accounts for 85% of the total accretion rate. For a kind of corn straw ash with high melting temperature, the proportion is only 37%. Compared with the actual slagging during biomass combustion, the modelling results can reflect a similar slagging situation on the surface of tube.*

Key words: biomass combustion, simulated ash, ash fusion, slagging, CFD modelling

### Introduction

Biomass, as a CO<sub>2</sub>-zero-emission RES, is attracting more and more attention. In China, over 130 dedicated biomass fired power plants have been operated, and it will account for 3% of the total power installed capacity with 30 GW by 2020 [1, 2]. The slagging problem in the furnace or on heating surface, however, can cause reduction of heat transfer efficiency

\* Corresponding author; e-mail: hzt@mail.xjtu.edu.cn

and damage on super-heaters, which impedes the utilization of biomass fuel severely [3, 4]. The slagging process concerns of the fuel property, combustion condition and heat transfer, which make it a complex physical-chemical problem. Ash fusion characteristics (AFC) is regarded as an important factor affecting the biomass furnace slagging [5, 6]. Compared to coal ash, biomass usually presents low ash fusion temperature (AFT) because of the high content of chlorine, Cl, and potassium, K. The softening temperature (ST) of wood biomass is on average 950 °C to 1000 °C, whereas that of straw biomass is about 1000 °C. For some seaweed biomass ST is less than 800 °C [7, 8]. The low AFT of biomass leads to adhesion and deposition of the ash, and further causes the slagging in furnace.

Li *et al.* [9] proposed that AFT could be an important criterion to choose the furnace exit temperature. The effect of ash composition on AFC was studied in their research. The result indicated that aluminum oxide ( $\text{Al}_2\text{O}_3$ ) increases initial deformation temperature (IDT) greatly. The base to acid ratio,  $R_{b/a}$ , was also used to help determine the slagging trend. An  $R_{b/a}$  value of 1.4 resulted in the lowest IDT of 800 °C. However, some other research indicated that the commonly used criteria of coal ash fusion slagging, such as  $R_{b/a}$ , silicon (Si) to aluminum (Al) ratio and slagging index, sometimes cannot reflect the slagging trend of biomass ash correctly [10, 11]. Thus, more research is needed to find the appropriate way to predicting biomass furnace slagging.

The CFD simulation is regarded as a proper method for slagging prediction, which can provide the detailed information of slag generation. Li *et al.* [12] investigated the slagging on a super-heater tube by CFD modelling. By taking deposition by inertial impaction into account, assuming all depositing particles are fully molten and the steam temperature in super-heater is constant, the slag model can provide thickness and surface temperature distributions of the flowing deposit layer, the temperature at the tube surface can also be calculated for choosing tube material. Besides, Garba *et al.* [13] studied the formation and growth of deposit on heating surfaces during co-combustion of biomass and coal by CFD modelling. The adhesion model was proposed on the basis of ash composition, AFT and viscosity curve, which gave a complete and detailed simulation and prediction of the slagging process.

It is generally considered that the deposition of biomass fly ash on heating surfaces is caused by the following mechanism: thermophoretic force, inertial impaction, ash fusion, *etc.* [13-15]. For the deposition caused by ash fusion, the viscosity of ash, which is determined by the ash composition and temperature, is regarded as an important index. The adhesion probability of ash corresponding to the viscosity will be employed in the modelling study. A study of a new integrated inertial collision fouling mechanism combined with suspended particle deposition and fouling removal has been reported by Pan *et al.* [15]. The developed model can accurately reconstruct the distribution of particulate deposition and the characteristic of fouling growth on boiler tubes.

However, little work has been done on simulation of biomass slagging, especially that combines the effect of the inertial impaction and molten ash adhesion of biomass ash particles on the slagging. Besides, the characteristics of molten ash are usually acquired from the database of thermodynamic equilibrium calculation software such as FactSage [16]. The actual AFC cannot be reflected precisely. Due to this situation, the AFC of self-made simulated biomass ashes have been studied in this research. The effect of four kinds of major ash composition on AFT has been discussed, and a CFD simulation has been performed based on the experiment results, to investigate how the AFC affect the deposition condition on tube wall of heating surfaces.

## Experimental study on AFC

### Methods and experimental apparatus

On basis of the investigation of the ash composition in several biomass-fired power plants in China,  $\text{Al}_2\text{O}_3$ , silicon dioxide ( $\text{SiO}_2$ ), calcium oxide ( $\text{CaO}$ ), and potassium oxide ( $\text{K}_2\text{O}$ ) together take over 50 wt.% of biomass ashes. So, the mixtures of these four materials are used as simulated biomass ashes. The effect of each component on the AFC and slagging potential is presented by means of ternary diagram after ash fusion test. Simulated biomass ashes are used to investigate the effects of  $\text{Al}_2\text{O}_3$ ,  $\text{SiO}_2$ ,  $\text{CaO}$ , and  $\text{K}_2\text{O}$  on AFC in detail.  $\text{K}_2\text{O}$  is made up by potassium chloride ( $\text{KCl}$ ) and potassium sulfate ( $\text{K}_2\text{SO}_4$ ) with a mole ratio of 3:1, based on the average value of S/Cl in the former investigation. Therefore, 5 kinds of analytical reagent (AR) have been prepared to compound the ash samples. Due to the relatively low content of Al, the mass fraction of  $\text{Al}_2\text{O}_3$  is set as 0, 3% and 7%. Under each percentage of  $\text{Al}_2\text{O}_3$ , the other components are mixed according to the condition arrangement in tab. 1 after normalization. Ash pyramids of all the samples have been made for ash fusion test.

The ash fusion test has been performed in an HR-8000B AFT analyzer. Heating rate is automatically controlled to 15 °C/min (0-900 °C) and 5 °C/min (900-1505 °C). The heat treatment of the ash pyramids has been done in atmosphere of air.

**Table 1. The mass fraction of components in simulated ashes**

$\text{Al}_2\text{O}_3$	$\text{SiO}_2:\text{CaO}:\text{K}_2\text{O}$				
0, 3%, 7%	0:0:8	0:1:7	0:2:6	0:3:5	0:4:4
	0:5:3	0:6:2	0:7:1	0:8:0	1:0:7
	1:1:6	1:2:5	1:3:4	1:4:3	1:5:2
	1:6:1	1:7:0	2:0:6	2:1:5	2:2:4
	2:3:3	2:4:2	2:5:1	2:6:0	3:0:5
	3:1:4	3:2:3	3:3:2	3:4:1	3:5:0
	4:0:4	4:1:3	4:2:2	4:3:1	4:4:0
	5:0:3	5:1:2	5:2:1	5:3:0	6:0:2
	6:1:1	6:2:0	7:0:1	7:1:0	8:0:0

### Results and discussion

Deformation temperature (DT) has been used to evaluate AFC of all ash samples. The DT distribution of simulated ashes at each percentage of  $\text{Al}_2\text{O}_3$  have been presented in fig. 1 by ternary diagrams. The ternary diagrams have been divided into three zones according to the temperature range: high temperature zone (HZ, >1400 °C), medium temperature zone (MZ, 900-1400 °C) and low temperature zone (LZ, <900 °C).

The DT distribution of simulated ashes with no Al is shown in fig. 1(a). DT decreases with increasing potassium (K). When content of K is over 50%, DT of ash sample belongs to LZ. Si and calcium (Ca) can significantly increase DT into HZ generally. However, DT moves from HZ into MZ when there are certain amounts of Si and Ca. It can be inferred that Si and Ca play as skeleton in ash respectively, which increase DT by supporting the structure of ash. While there are certain contents of K, Ca, and Si, low temperature eutectic reactions occur and form low melting products, which decrease DT into MZ.

Ash samples present different AFC with the addition of  $\text{Al}_2\text{O}_3$ , which can be seen in figs. 1(b) and 1(c). The following comparisons have been made among the corresponding conditions with different content of Al (0, 3%, and 7%). When the mass fraction of  $\text{Al}_2\text{O}_3$  is increased from 0 to 3%, DT is seemed to be higher generally due to the skeleton effect of  $\text{Al}_2\text{O}_3$ . While the ash samples consist of low content of K with high content of Ca and Si, DT has been observed to decrease because of the promotion of eutectic reactions by Al. Besides, an obvious reduction of LZ and HZ has been shown in fig. 2(c), which means the addition of  $\text{Al}_2\text{O}_3$  decreases DT when contents of Si and Ca are high and increases DT when content of K is high.

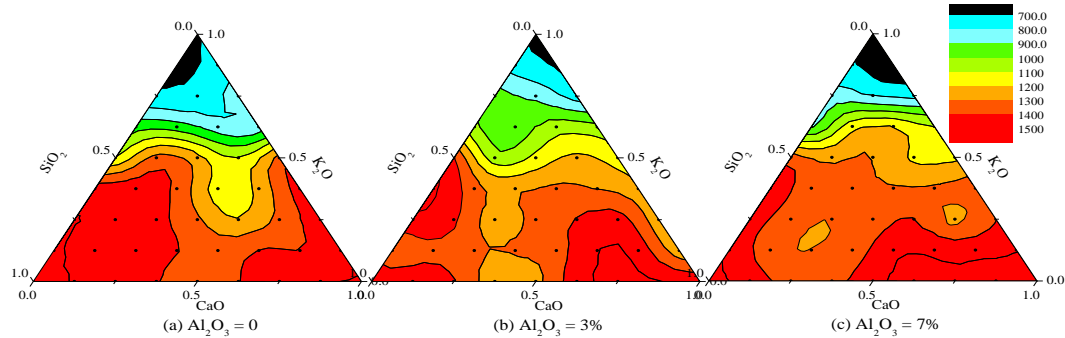


Figure 1. The DT distribution of simulated ashes  
(for color image see journal web site)

## Numerical models

### Molten ash adhesion model

The pictures recording the continuous change of the ash pyramid shape can be acquired from ash fusion test. On the assumption that the ash samples are regular triangular pyramids, the sectional area,  $S$ , and base length,  $d$ , can be identified in the picture, and thus the volume of ash pyramid,  $V$ , can be approximately calculated:

$$V = \sqrt{3}dS/6 \quad (1)$$

According to the work of Kaer [17], the ash sample is non-sticky if the mass fraction of molten phase is below 15%. When it is between 15% and 70%, it is assumed to be sticky and easy to form deposits. Above this percentage, it is assumed to be flowing and thus non-sticky again. On the assumption that the density of ash pyramids does not change with the increase of temperature, the mass of ash pyramid is in proportion to the volume. Therefore, the ash is sticky and easy to adhere to the tube wall of heating surfaces when the relative volume of ash pyramid ranges from 85-30%. The corresponding temperatures  $T_{85\%}$  and  $T_{30\%}$  at which the relative volume of 85% and 30% are selected as characteristic temperatures.

For the biomass ash samples of different composition, the characteristic temperatures of ash molten adhesion have been identified from the ash fusion test. On consideration of the interaction between different reactants, the relation between characteristic temperatures and ash compositions has been calculated using nonlinear regression method. The calculation is done using the mass fractions of  $\text{SiO}_2$ ,  $\text{CaO}$ , and  $\text{K}_2\text{O}$ , while the effect of Al is acquired by linear interpolation. The expressions of the characteristic temperatures can be obtained:

$$T_{85\%} = a_0 + a_1w_1 + a_2w_2 + a_3w_3 + a_{12}w_1w_2 + a_{13}w_1w_3 + a_{23}w_2w_3 + a_4w_1w_2w_3 \quad (2)$$

$$T_{30\%} = b_0 + b_1w_1 + b_2w_2 + b_3w_3 + b_{12}w_1w_2 + b_{13}w_1w_3 + b_{23}w_2w_3 + b_4w_1w_2w_3 \quad (3)$$

where  $w_1$ ,  $w_2$ , and  $w_3$  refer to the mass fractions of  $\text{SiO}_2$ ,  $\text{CaO}$ , and  $\text{K}_2\text{O}$ . The coefficients in eq. (2) and eq. (3) are obtained by fitting calculation. For other mass fraction of Al between 0 to 7%, interpolation has been used for characteristic temperatures calculation. By these data the characteristic temperatures of ash with any content of  $\text{Al}_2\text{O}_3$ ,  $\text{SiO}_2$ ,  $\text{CaO}$ , and  $\text{K}_2\text{O}$  can be acquired and employed as the criterion of adhesion. The adhesion probability  $\eta_{\text{ad}}$  can be calculated by:

$$\eta_{ad} = \begin{cases} \frac{T_p - T_{85\%}}{T_{30\%} - T_{85\%}}, & T_{85\%} \leq T_p \leq T_{30\%} \\ 0, & T_p < T_{85\%} \text{ or } T_p > T_{30\%} \end{cases} \quad (4)$$

where  $T_p$  represents the temperature of ash particles.

#### *Deposition model of inertial impaction*

Pan *et al.* [15] proposed an integrated theoretical fouling model to simulate the deposition of inertial impaction on tube wall of heating surfaces. Based on Kern-Seaton theory, the model takes both inertial impaction deposition and suspended particle deposition removal mechanism into consideration. According to this deposition model, when an oblique incident particle slips along the surface, a critical sticking angle can then be defined:

$$\tan \theta_{cr} = \frac{V_{it}}{V_{in}} = \sqrt{\frac{Q_{it}}{Q_{in}}} = \frac{\mu^*}{(32\beta^3)^{1/2}} \sqrt{\frac{E^*}{G^*}} \quad (5)$$

where  $\mu^*$  is an effective friction coefficient,  $\beta$  is the effective coefficient of the contact radius.  $E^*$  and  $G^*$  are the effective elastic and shear modulus of the particle-granules collision, relatively.

When the stored elastic energy equals to the interfacial adhesive energy, the normal velocity is defined as critical rebounding velocity,  $V_{dn\_cri}$ . Combining the critical sticking angle and the critical rebounding velocity, the deposition criterion of inertial impaction has been setup.

From the above, criteria for inertial impact fouling can be described:

- if  $\theta' > \theta_{cr}$ , sticking occurs irrespective of particle velocity, and
- if  $\theta' \leq \theta_{cr}$  and  $V_{in} \leq V_{dn\_cri}$ , deposition of particle occurs.

#### **The CFD modelling and discussion**

Based on the proposed model, a 3-D simulation of the deposition on the tube of heating surface has been developed with FLUENT 6.3.26. To simplify the simulation, a length of a tube from superheater and the zone nearby has been selected as the computed field. The parameters of the ash particles and flue gas are taken from operating conditions of power plants: the inlet temperature and velocity of flue gas are 1173 K and 10 m/s, respectively, the temperature of tube wall is 773 K, the mass flow rate of fly ash particles is  $10^{-5}$  kg/s. The diameter distribution follows the Rosin-Rammler rule with sizes from 10  $\mu\text{m}$  to 150  $\mu\text{m}$ . The flow field has been generated with non-structured mesh. Eulerian-Lagrangian equations, the turbulence  $k$ - $\varepsilon$  model, and the semi-implicit method for pressure linked equations-consistent (SIMPLEC) algorithm are employed for the calculation of particle-loaded flue gas flow. Besides, based on the proposed model, a user defined function has been developed using the macro of DEFINE\_DPM\_EROSION to execute the inertial impaction and molten ash adhesion mechanism.

The composition of ash particles is selected on basis of the ash composition of Xinjiang cotton straw (XCS) and Henan corn straw (HCS). The relative contents of  $\text{Al}_2\text{O}_3$ ,  $\text{SiO}_2$ ,  $\text{CaO}$ , and  $\text{K}_2\text{O}$  are listed in tab. 2.

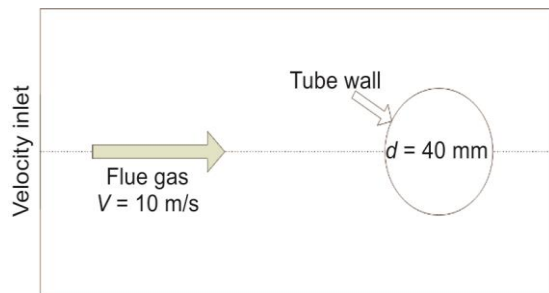
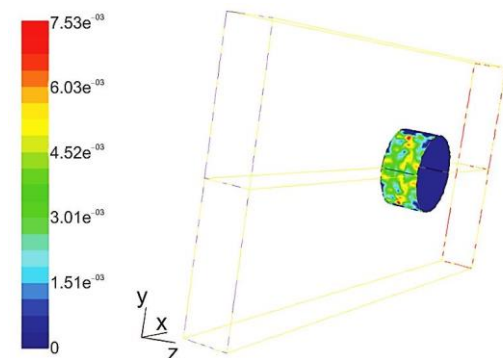
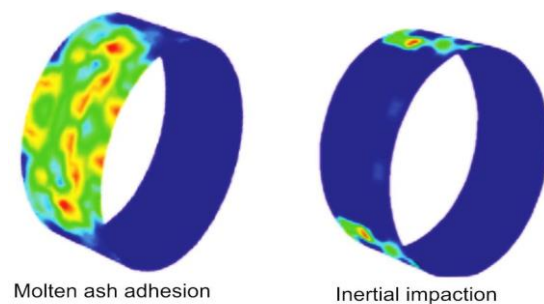
The computed field has been shown in fig. 2.

Simulation results of deposition of XCS ash particles have been shown in fig. 3.

The accretion rate on tube surfaces is composed of two parts: molten ash adhesion and inertial impaction, the effects of which have been presented in fig. 4.

**Table 2. Normalized contents of  $\text{Al}_2\text{O}_3$ ,  $\text{SiO}_2$ ,  $\text{CaO}$  and  $\text{K}_2\text{O}$  in ashes**

	$\text{Al}_2\text{O}_3$ [%]	$\text{SiO}_2$ [%]	$\text{CaO}$ [%]	$\text{K}_2\text{O}$ [%]
XCS	5.89	20.11	36.82	37.18
HCS	7.00	69.92	8.12	14.96

**Figure 2. Computed field****Figure 3. Accretion rate of XCS ash particles ( $\text{kgm}^{-2}\text{s}^{-1}$ )**  
(for color image see journal web site)**Figure 4. Accretion rate of molten ash adhesion and inertial impaction (XCS,  $\text{kgm}^{-2}\text{s}^{-1}$ )**

In fact, when a biomass-fired power plant in northwest China used the XCS for direct combustion, the boiler was facing severe slagging problem. The deposits on the surfaces of superheaters, which required cleaning every 20-30 days, have been presented in fig. 7(a) [1].

The area-weighted average value of accretion rate has been calculated as  $1.30 \cdot 10^{-3} \text{ kg/m}^2\text{s}$ , while the accretion rate of molten ash adhesion and inertial impaction are  $1.10 \cdot 10^{-3} \text{ kg/m}^2\text{s}$  and  $2.09 \cdot 10^{-4} \text{ kg/m}^2\text{s}$ , respectively.

From these results, it is indicated that the ash fusion process played a dominant role during the deposition in this case. The accretion rate of molten ash adhesion accounts for 85% of the total rate. Due to the high content of Ca and K, the AFT of XCS ash are relatively low. The molten ash adhesion occurs easily at high temperature. Besides, the adhesion of molten ash particles occurs all over the windward side, while the deposition of impaction occurs at the top/bottom zone of the windward side. It is because the deposition of inertial impaction depends on particle normal velocity and impact angle. Therefore, it is difficult for the ash particles to deposit at the middle part of the windward side of tube due to the high velocity.

Simulation results of deposition of HCS ash particles have been shown in fig. 5. The area-weighted average value of accretion rate has been calculated as  $3.33 \cdot 10^{-4} \text{ kg/m}^2\text{s}$ , while the accretion rate of molten ash adhesion and inertial impaction are  $1.26 \cdot 10^{-4} \text{ kg/m}^2\text{s}$  and  $2.07 \cdot 10^{-4} \text{ kg/m}^2\text{s}$ , respectively.

The accretion rate distribution of molten ash adhesion and inertial impaction have been shown in fig. 6. The accretion rate of molten ash adhesion accounts for only 37% of the total rate.

These two biomass ashes present similar trends and rate of inertial impaction. However, HCS ash has high fusion temperatures because of the high contents of Si and Al, and thus can relieve the deposition by molten ash adhesion.

Therefore, the deposition of XCS ash on the surface of superheater tube has been modelled. According to the calculated accretion rate, the shape of deposits after 72 hours has been shown in fig. 7(b).

Compared with the actual slagging, this model can partially reflect the slagging situation on tube wall with similar shape and larger amount of deposits. Because of a larger normal velocity, rebounding of the particles occurs, leading to different shapes at the top of the deposits in the modelling result. Besides, the mechanism of target particle removal has not been added into the model. With specific incident velocity and angle, the incident particle can remove the target particles in the existing deposits, which will reduce the deposition amount and change the shape of slag. This will be considered in our future work.

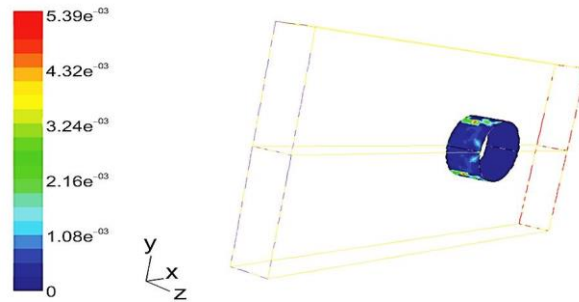


Figure 5. Accretion rate of HCS ash particles ( $\text{kgm}^{-2}\text{s}^{-1}$ )  
 (for color image see journal web site)

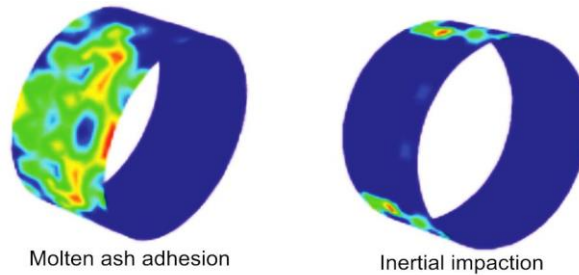
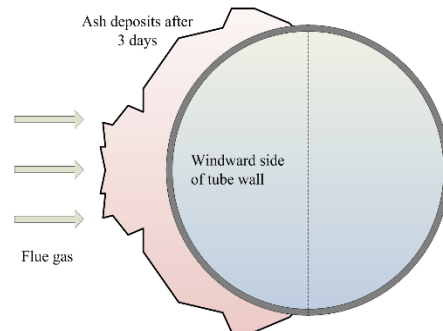


Figure 6. Accretion rate of molten ash adhesion (HCS,  $\text{kgm}^{-2}\text{s}^{-1}$ )



(a)



(b)

Figure 7. Slagging on the tube wall of superheaters (a) and modelling results for a 3-day deposition (b)

### Conclusions

In this study, based on the basic ash composition of biomass, the mixture of  $\text{SiO}_2$ ,  $\text{CaO}$ ,  $\text{K}_2\text{O}$ , and  $\text{Al}_2\text{O}_3$  have been selected as simulated ashes for ash fusion test. The results indicate that DT decreases with increased  $\text{K}_2\text{O}$ .  $\text{CaO}$  and  $\text{SiO}_2$  in the ash have skeleton effect and lead to high DT, but the interaction of  $\text{K}_2\text{O}$ ,  $\text{CaO}$  and  $\text{SiO}_2$  decreases DT because of the low-temperature eutectic reactions.  $\text{Al}_2\text{O}_3$  has a two-way effect on DT. When K content is high, it increases DT by forming Si-Al-K compounds. When Ca or Si content is high, it decreases DT by forming Si-Al-Ca compounds.

Besides, the characteristic temperatures for the molten ash adhesion have been acquired from experimental data and post-processing. Combined with a deposition model of inertial impaction, an integrated model of ash particle deposition has been developed. A modelling study of the deposition on the surface of superheater tube has been performed. The results indicated that ash fusion process affects the slagging significantly. For the cotton straw ash with high content of Ca and K, the accretion rate can reach up to  $1.30 \cdot 10^{-3} \text{ kg/m}^2\text{s}$ . The accretion rate of molten ash adhesion is  $1.10 \cdot 10^{-3} \text{ kg/m}^2\text{s}$ , which accounts for 85% of the total rate, indicating the importance of ash melting during slagging.

Based on the calculated rate, the modelling result of a 3-day deposition has been presented. Compared with the actual slagging during biomass combustion, the deposition by inertial impaction hardly occurs at the middle part due to the high particle velocity while molten ash adhesion occurs all over the windward side of tube. The modelling results can partially reflect the slagging situation with similar shape and larger amount of deposits. The discrimination may be reduced by adding the mechanism of target particle removal into the model in the future work.

### Acknowledgment

The present work was supported by the National Key Research and Development Plan of China (No. 2016YFB0601504).

### References

- [1] Niu, Y., et al., Slagging Characteristics on the Superheaters of a 12 MW Biomass-Fired Boiler, *Energy & Fuels*, 24 (2010), 9, pp. 5222-5227
- [2] Reichelt, J., et al., Formation of Deposits on the Surfaces of Superheaters and Economisers of MSW Incinerator Plants, *Waste Management*, 33 (2013), 1, pp. 43-51
- [3] Vassilev, S. V., et al., Influence of Mineral and Chemical Composition of Coal Ashes on Their Fusibility, *Fuel Processing Technology*, 45 (1995), 1, pp. 27-51
- [4] Zhu, Y., et al., Short Review on the Origin and Countermeasure of Biomass Slagging in Grate Furnace, *Frontiers in Energy Research*, 2 (2014), Feb., p. 7
- [5] Melissari, B., Ash Related Problems with High Alkali Biomass and its Mitigationexperimental Evaluation, *Memoria Investigaciones en Ingenieria*, 12 (2014), Aug., pp. 31-44
- [6] Niu, Y., et al., Ash-Related Issues During Biomass Combustion: Alkali-Induced Slagging, Silicate Melt-Induced Slagging (Ash Fusion), Agglomeration, Corrosion, Ash Utilization, and Related Countermeasures, *Progress in Energy and Combustion Science*, 52 (2016), Feb., pp. 1-61
- [7] Heinzel, T., et al., Investigation of Slagging in Pulverized Fuel Co-combustion of Biomass and Coal at a Pilot-Scale Test Facility, *Fuel Processing Technology*, 54 (1998), 1, pp. 109-125
- [8] Llorente, M. F., Garcia, J. C., Comparing Methods for Predicting the Sintering of Biomass Ash in Combustion, *Fuel*, 84 (2005), 14, pp. 1893-1900
- [9] Li, Q., et al., Study on Ash Fusion Temperature Using Original and Simulated Biomass Ashes, *Fuel Processing Technology*, 107 (2013), Mar., pp. 107-112
- [10] Masia, A. T., et al., Characterising Ash of Biomass and Waste, *Fuel Processing Technology*, 88 (2007), 11, pp. 1071-1081
- [11] Niu, Y., et al., Fusion Characteristics of Capsicum Stalk Ash, *Asia-Pacific Journal of Chemical Engineering*, 6 (2011), 4, pp. 679-684
- [12] Li, B., et al., CFD Investigation of Slagging on a Super-heater Tube in a Kraft Recovery Boiler, *Fuel Processing Technology*, 105 (2013), Jan., pp. 149-153
- [13] Garba, M., et al., Prediction of Potassium Chloride Sulfation and Its Effect on Deposition in Biomass-Fired Boilers, *Energy & Fuels*, 26 (2012), 11, pp. 6501-6508
- [14] Wang, H., Harb, J. N., Modeling of Ash Deposition in Large-scale Combustion Facilities Burning Pulverized Coal, *Progress in Energy and Combustion Science*, 23 (1997), 3, pp. 267-282
- [15] Pan, Y., et al., An Integrated Theoretical Fouling Model for Convective Heating Surfaces in Coal-fired Boilers, *Powder Technology*, 210 (2011), 2, pp. 150-156



- 
- [16] Yang, X., *et al.*, Understanding the Ash Deposition Formation in Zhundong Lignite Combustion through Dynamic CFD Modelling Analysis, *Fuel*, 194 (2017), Apr., pp. 533-543
- [17] Kær, S. K., Numerical Investigation of Ash Deposition in Straw-Fired Boilers: Using CFD as the Framework for Slagging and Fouling Predictions, Ph. D. thesis, Aalborg University, Aalborg, Denmark, 2001